Equilibrium flow shear and magnetic shear effect on zonal flow generation and toroidal mode coupling

S. Tokunaga 1), M. Yagi 2,3), S.-I. Itoh 2), K. Itoh 2,4)

1) WCI Center for Fusion Theory, National Fusion Research Institute, Daejeon Korea
2) Research Institute for Applied Mechanics, Kyushu University, Kasuga, Japan
3) Japan Atomic Energy Agency, Naka, Japan
4) National Institute for Fusion Science, Toki, Japan

E-mail contact of main author: toku@nfri.re.kr

Abstract. Magnetic shear effect on spontaneous flow generation in reversed shear plasmas is investigated based on global gyro-fluid ITG simulations. Off-resonant modes around q-minimum region are taken into account as well. The excitation of off-resonant mode due to the toroidal mode coupling is observed in the nonlinear saturation phase. Intermittent growth of zonal flow in a case with relatively flat negative magnetic shear is observed. In the flat negative shear case, intermittent burst with a long period occurs besides small-scale avalanche around q-minimum. The burst propagates large extent in the radial direction, and contributes to the enhancement of zonal flow in the vicinity of q-minimum position. In the strong turbulent state, the magnetic shear affects on the flow generation by means of the nonlocal and intermittent turbulent transport.

1. Introduction

Understanding of internal transport barrier (ITB) [1] formation mechanism is one of the most crucial issues to establish advanced operation scenario in ITER or the other modern magnetic confinement devices. So far a number of experimental, theoretical and simulation studies have been dedicated, and our understanding of ITB has made significant progress [2, 3].

Mean ExB flow shearing [2, 4], negative magnetic shear and magnetic well [5], negative magnetic shear [6], rational surface gap in zero-shear region [7], zonal flow [8], and selective turbulence spreading [9], Geodesic Acoustic Mode (GAM)[10], etc., have been reported as possible factors of ITB formation. However, fully dynamical spontaneous formation of ITB has not been simulated by direct simulation. Theoretical understanding of whole mechanism and needed condition for barrier formation has not been fully revealed. Though equilibrium ExB flow shear is widely recognized as the most plausible player in ITB formation, dynamical explanation of growth of radial electric field has not been given. Recent experimental studies show that poloidal rotation profile in triggering event of ITB formation does not agree with neo-classical estimation (excursion) [11,12]. Linear stabilization of ion temperature gradient driven drift wave (ITG) mode by negative magnetic shear and self-regulation of ITG mode by zonal flow generation are important in turbulence simulation but not so strong as to be responsible in internal barrier formation by alone. Zero-shear gap around q-minimum region in reversed magnetic shear configuration is also effective feature to provide quiescent region in vicinity of q-minimum position when we neglected off-resonant modes, i.e. modes do not have rational magnetic surface in plasma.

However, it has been argued that, off-resonant modes are excited around q-minimum region and the envelope of ballooning mode smoothly provides anomalous transport over the zero-shear gap. Such ITG mode in flat shear region had been investigated by the use of global gyro-kinetic simulation and was found to be "slab-like" [13]. It was also observed that even in the absent of off-resonant micro-mode, meso-scale off-resonant mode can grow over the gap and destroys the barrier-like structure [14].

In the present work, we report the magnetic shear effect on flow generation in the strong turbulent state. Off-resonant modes around q-minimum are taken into account and heat source simulation is performed. Magnetic shear effect on the excitation of off-resonant mode due to the toroidal mode coupling is investigated. Intermittent growth of zonal flow in a case with relatively flat magnetic shear is observed. In the flat shear case, larger-scale intermittent burst is caused by ITG turbulence followed by the temperature profile modification by avalanche. It is found that, the enhancement of zonal flow is attributed to nonlocal and intermittent turbulent transport.

2. Simulation Model

We employ 3-field electrostatic gyro-Landau-fluid model to investigate ITG turbulence around q-minimum region considering off-resonant modes as well [9,15-18]. Heat source simulation is performed with a source profile in the quadratic form. Four safety factor profiles with the same q-minimum (q_min=1.35) and different magnetic shear in core region (r<0.6) are examined.

2.1. Set of Model Equations

The model consists of Vorticity equation coupled with continuity equation, parallel momentum equation and ion temperature evolution equation;

$$\frac{d\tilde{w}}{d\bar{t}} + \kappa_{\hat{n}}\bar{\nabla}_\theta\tilde{\Phi} - 2\varepsilon_a\omega_d\tilde{F} = -\rho_*^2\bar{\mu}\bar{\nabla}_\perp^4\tilde{F} + \rho_*\frac{q}{\varepsilon}\bar{\mu}^{NC}\frac{1}{\bar{r}}\frac{\partial(\bar{r}U_p)}{\partial\bar{r}} - \frac{\varepsilon_a}{\rho_*}\bar{\nabla}_\|\tilde{V}_\| \tag{1}$$

$$\frac{d\tilde{V}_\|}{d\bar{t}} = 4\bar{\mu}\bar{\nabla}_\perp^2\tilde{V}_\| + \bar{\mu}^{NC}U_p - \frac{2}{5}\frac{\sqrt{\pi}}{\rho_*}\varepsilon_a\sqrt{\frac{1}{\tau}}\left|\bar{\nabla}_\|\right|\tilde{V}_\| + \frac{2}{5}\frac{\varepsilon_a}{\rho_*}\frac{1}{\tau}\bar{\nabla}_\|\tilde{T} - \frac{\varepsilon_a}{\rho_*}\bar{\nabla}_\|\tilde{F} \tag{2}$$

$$\frac{3}{2}\left(\frac{d\tilde{T}}{d\bar{t}} + \kappa_{\hat{T}}\bar{\nabla}_\theta\tilde{\Phi}\right) - \left(\frac{d\tilde{n}}{d\bar{t}} + \kappa_{\hat{n}}\bar{\nabla}_\theta\tilde{\Phi}\right) = \bar{\chi}_\perp\bar{\nabla}_\perp^2\tilde{T} - \frac{9}{5}\frac{\varepsilon_a}{\sqrt{\pi}\rho_*}\sqrt{\frac{1}{\tau}}\left|\bar{\nabla}_\|\right|\tilde{T} + \frac{2}{5}\frac{\varepsilon_a}{\rho_*}\bar{\nabla}_\|\tilde{V}_\| \tag{3}$$

where,

$$\tilde{w} = \tilde{n} - \rho_*^2\bar{\nabla}_\perp^2\tilde{F} \qquad \tilde{F} = \tilde{\Phi} + \frac{\tilde{p}}{\tau} \qquad \tilde{p} = \tilde{n} + \tilde{T} \qquad \tilde{n} = \tilde{\Phi} - \langle\tilde{\Phi}\rangle$$

$$\omega_d = \cos\theta\frac{1}{\bar{r}}\frac{\partial}{\partial\theta} + \sin\theta\frac{\partial}{\partial\bar{r}} \qquad U_p = \tilde{V}_\| + \rho_*\frac{q}{\varepsilon}\frac{\partial\tilde{F}}{\partial\bar{r}} \qquad \bar{\nabla}_\| = \frac{1}{q}\left(q\frac{\partial}{\partial\bar{z}} + \frac{\partial}{\partial\theta}\right)$$

$$\kappa_{\hat{n}} = -\frac{d\hat{n}}{d\bar{r}} \qquad \kappa_{\hat{T}} = -\frac{d\hat{T}}{d\bar{r}} \qquad \varepsilon_a = \frac{a}{R_0} \qquad \varepsilon = \frac{r}{R_0} \qquad \rho_* = \frac{\rho_s}{a}$$

The adiabatic electron response is assumed for simplicity. Toroidal effect is included via curvature operator ω_d into cylindrical geometry. Normalization is taken as,

$$\left(\frac{t}{a^2/\chi_B}, \frac{r}{a}, a\nabla_\perp, R_0\partial/\partial z\right) \to \left(\bar{t}, \bar{r}, \bar{\nabla}_\perp, \partial/\partial\bar{z}\right)$$,where $\chi_B = \frac{T_{e0}}{eB} = \rho_s c_s$ is Bohm diffusion coefficient.

$$\left(\frac{n_1}{n_0}, \frac{n_{eq}}{n_0}, \frac{\Phi_1}{T_0/e}, \frac{V_{\|1}}{c_s}, \frac{T_1}{T_0}, \frac{T_{eq}}{T_0}\right) \to \left(\tilde{n}, \hat{n}, \tilde{\Phi}, \tilde{V}_\|, \tilde{T}, \hat{T}\right)$$ and $\frac{t_B}{a^2}\left(\frac{\mu}{m_in_0}, \chi_\perp, a^2\mu^{NC}\right) \to \left(\bar{\mu}, \bar{\chi}_\perp, \bar{\mu}^{NC}\right)$.

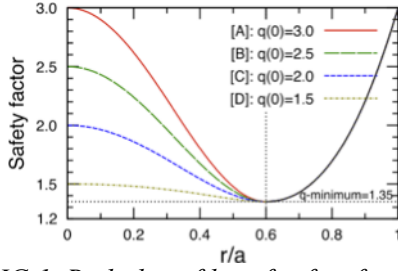## 2.2. Initial Profiles and Heat Source Term
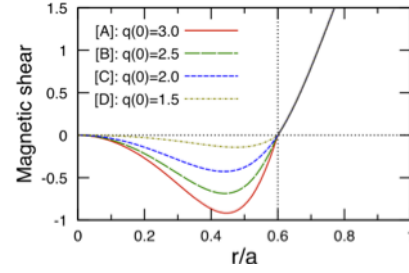

FIG.1. Radial profiles of safety factor q.

FIG.2. Radial profiles of magnetic shear.

To investigate the magnetic shear effect on ITG turbulence, reversed magnetic shear profiles given by Ref. [19] with a common *q*-minimum value *q_min=1.35* at *r/a=0.6* are introduced combining different magnetic shear in the core region. FIG. 1 and 2 indicate the reversed shear q profile and the corresponding magnetic shear, respectively. These In the outside region of *q*-minimum position, $r/a \geq 0.6$, they are identical. Because of the stabilizing effect of negative magnetic shear on ITG modes, especially the linear threshold is significantly different among four cases.

No density flux is generated due to the adiabatic electron response so that the equilibrium density profile $n(\bar{r}) = (1 - \bar{r}^2)/(1 - \bar{r}_s^2)$ is fixed, where $\bar{r} = r/a$ and $\bar{r}_s = 0.6$.

Heat source is given by the quadratic form, $S_{T_i}(\bar{r}) = -4 \times 10^{-3}(2\bar{r}^2 - 1)^2/(1 - \bar{r}_s^2)^2$. It is added in to the R.H.S of the ion temperature evolution equation. Note that this type of source profile provides the heat sink in edge region. In our model, the ion temperature cannot be divided into equilibrium and fluctuating quantities, but is rather solved as a whole.

The value of $\rho*$ is given as 0.01 in this study.

2.3. Numerical Settings

Off-resonant modes are taken into account: *1.2 <m/n< q_min=1.35* are included as shown in FIG. 3, where *m* is poloidal mode number, and *n* is toroidal mode number.

3. Simulation Results

3.1. Off-resonant Mode

FIG.3. Calculated modes in the case with q0=3.0 in m-n space.

In this section, we discuss on the off-resonant mode excitation in the saturation phase. Multiplying complex conjugate of F, to the eq. (1), we obtain the electrostatic energy conservation equation as

$$\frac{1 + \tau}{\tau} \frac{1}{2} \frac{\partial}{\partial t} \langle |\Phi_{m,n}|^2 \rangle + \left\langle \frac{T_{m,n}^*}{\tau} \frac{\partial}{\partial t} \Phi_{m,n} \right\rangle + \frac{1}{2} \rho_*^2 \frac{\partial}{\partial t} \left\langle \left| \frac{\partial F_{m,n}}{\partial r} \right|^2 + k_y^2 |F_{m,n}|^2 \right\rangle$$

$$= \langle F_{m,n}^*[\Phi, \rho_*^2 \nabla_\perp^2 F]_{m,n} \rangle - \langle \kappa_n F_{m,n}^* i \frac{m}{r} \Phi_{m,n} \rangle - A \langle F_{m,n}^* i k_{\parallel m,n} V_{\parallel m,n} \rangle$$

$$+ i\epsilon \left\langle F_{m,n}^* \left(\frac{m+1}{r} F_{m+1,n} + \frac{m-1}{r} F_{m-1,n} \right) \right\rangle + i\epsilon \left\langle F_{m,n}^* \left(\frac{\partial}{\partial r} F_{m+1,n} - \frac{\partial}{\partial r} F_{m-1,n} \right) \right\rangle$$

$$+ \rho_* \frac{q}{\epsilon} \mu^{NC} \left\langle F_{m,n}^* \frac{1}{r} \frac{\partial r U_{pm,n}}{\partial r} \right\rangle - \rho_*^2 \mu \langle |\nabla_\perp^2 F_{m,n}|^2 \rangle.$$

The 1st term of the R.H.S indicates the energy transfer to a mode (m,n) due to the nonlinear coupling (Reynolds stress) and the 4th and 5th term are corresponding to the energy transfer
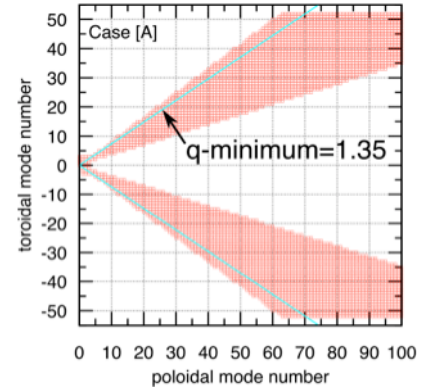
via toroidal mode coupling. Estimating these term, we investigated the excitation mechanism of an off-resonant mode. We chose the modes with the same toroidal mode number as n=34 but different poloidal mode number, which compose one of the strongest ITG mode(ballooning mode) around q-minimum region in the saturation phase. Here, $m \geq 46$ are resonant modes, and m<46 are off-resonant. FIG. 4 shows the temporal evolution of energy transfer via toroidal mode coupling and fluctuating electrostatic energy for the (44,34)-(47,34) modes. We also check the amplitude of energy transfer channel for nonlinear coupling and three-wave coupling with (1,0), i.e. $(m \pm 1, n) \mp (1,0) \Rightarrow (m,n)$. It is found that their contributions are much smaller than the toroidal mode coupling itself (less than 0.1%).
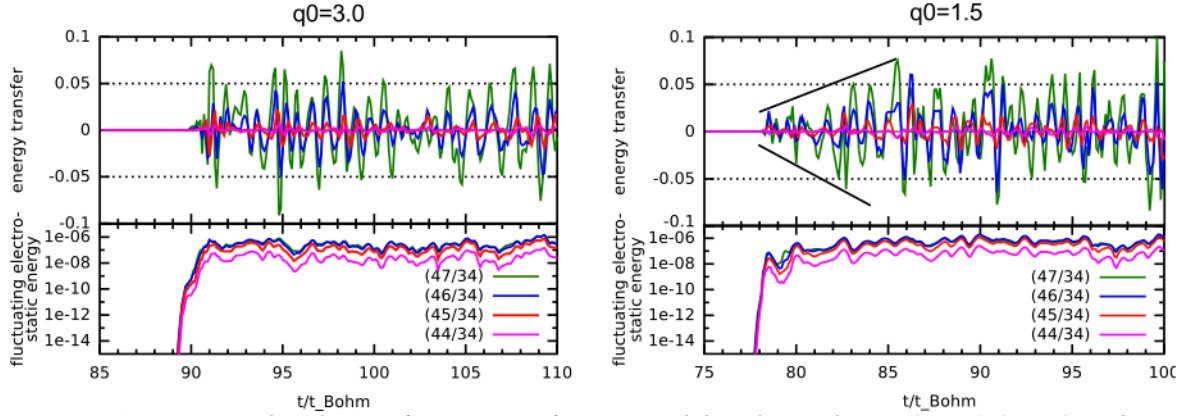

FIG. 4. Temporal evolution of energy transfer via toroidal mode coupling to (47,34)-(45,34) mode and fluctuating electrostatic energy integrated over r, in the case with q0=3.0 and q0=1.5.

As shown in FIG. 4, the energy transfer via toroidal mode coupling becomes large after the saturation. However, in the case with q0=1.5, it is less effective at the beginning of the saturation phase (79<t<85). Namely, they are "slab-like" mode structure in this stage. After that, toroidal coupling is getting strong gradually. Finally, in the fully nonlinear phase (85<t), mode gap around q-minimum region does not suppress the ballooning mode any more.
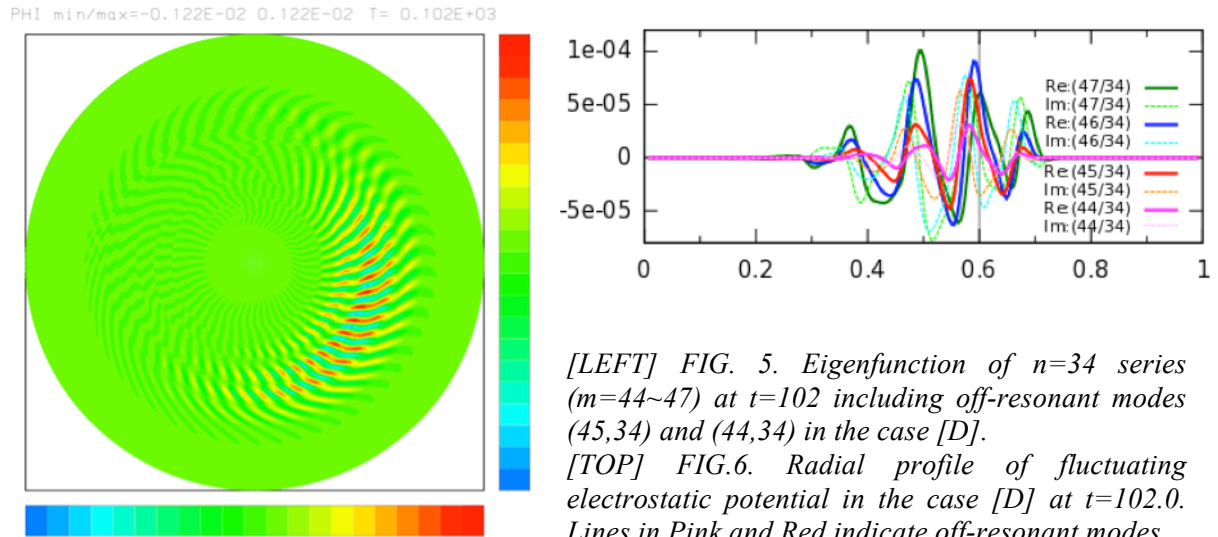
[LEFT] FIG. 5. Eigenfunction of n=34 series (m=44~47) at t=102 including off-resonant modes (45,34) and (44,34) in the case [D].
[TOP] FIG.6. Radial profile of fluctuating electrostatic potential in the case [D] at t=102.0. Lines in Pink and Red indicate off-resonant modes.

FIG. 5 shows a snap shot of eigenfunction of phi of n=34 and m=44~47 component at t=102.0. The time is corresponding to the instance when the turbulence is relatively quiescent. The eigenfunction clearly indicates ballooning mode structure. FIG. 6 gives each eigenfunction at the same time. (44,34) and (45,34) in red and pink lines imply that they are

strongly coupled with resonant modes via toroidal mode coupling. Off-resonant mode around q-minimum region is slab-like in linear phase, however, in the fully nonlinear phase, they compose the toroidal ITG mode.

3.2 Zonal flow generation

The Contour plot shown in FIG. 7 presents temporal evolution of radial profile of zonal component of V$_{ExB}$ with short radial wavelength ($10\rho*$). The measure of color chart is common for the all cases.

  In each case, frequent outward propagation of zonal flow in the short timescale is clearly shown. In addition, in the case [C] (q0=2.0) and [D] (q0=1.5) indicate, intermittent oscillation of ExB flow around r~0.6 in longer-timescale. Hereafter, we call the former one as small avalanche. In this section, we will focus on the case [D] with q0=1.5. It should be noted again that q profile is identical in the region r>0.6 for all cases.
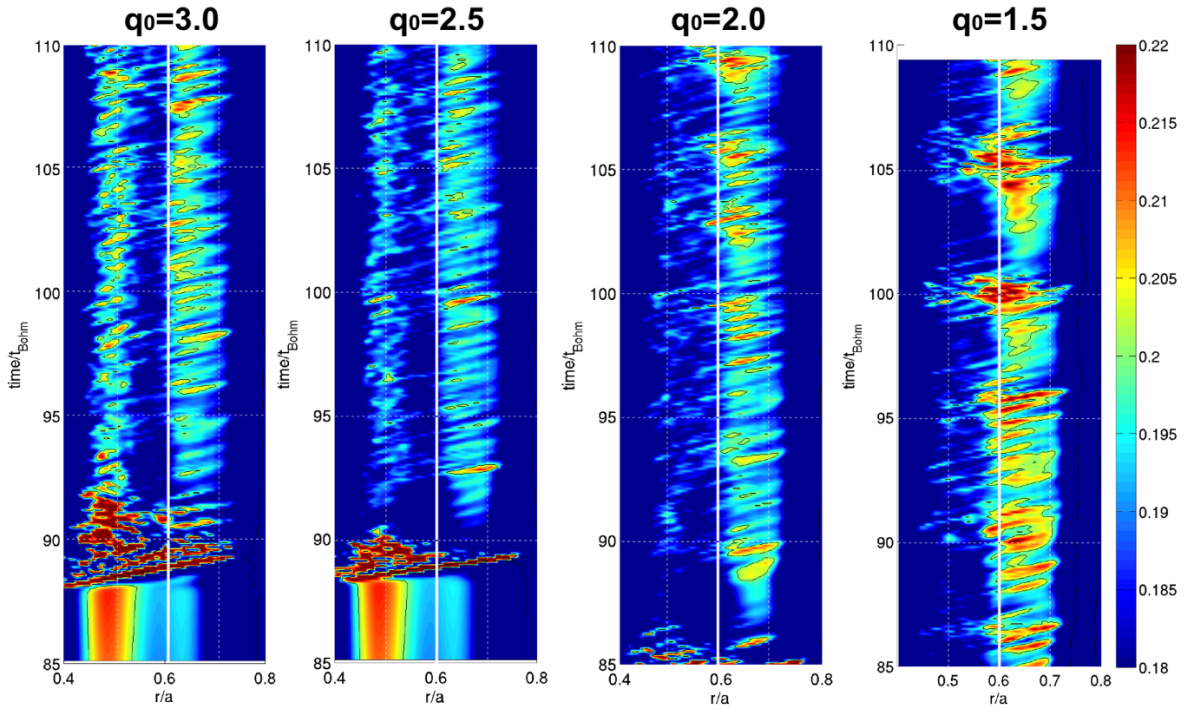

FIG. 7. Temporal evolution of radial profile of V_{ExB} with short k_r component.

The period of small avalanche is roughly Δt~0.5(Bohm time) and it occurs around r/a~0.65, on the other hand, the period of large-scale burst is roughly Δt~5(Bohm time) and the center is located at the q-minimum position.
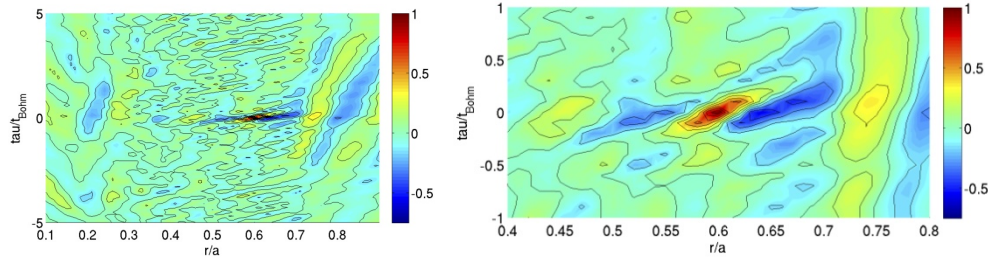

FIG. 8. [Left] Contour plots of cross-correlation coefficient: $\rho_{x,x=0.6}(\tau) \equiv R_{x,0.6}(\tau)\big/\big(R_{0.6,0.6}(0)R_{xx}(0)\big)^{1/2}$ for fluctuating component of $E_r^{0,0}$ with short k_r (zonal flow) and [Right] extended view around r=0.6 area.

FIG. 8 shows contour plot of spatial correlation coefficient among $\tilde{E}_r^{0,0}(r)$ and $\tilde{E}_r^{0,0}(0.6)$. Outward propagation of zonal electric field from r~0.45 to r~0.7 is shown. It is seen that the propagation speed does not strongly depend on magnetic shear. However, the correlation length is getting longer as the shear becomes weaker. The figure also indicates that, the auto-correlation time is small. The zonal flow propagation occurs intermittently. Though this small avalanche is clear in the contour of correlation of Er, it is hardly seen in the temperature channel, especially in the inner region from r=0.6.

3.3 Long-time scale variation

FIG. 9 shows temporal evolution of L_T^{-1} profile. It is found that, the intermittent enhancement of ExB occurs synchronizing with the large-scale temperature profile relaxation. The equilibrium part of radial electric field is also varying in this timescale. Namely, the large burst is related with the equilibrium state and it is separated from the turbulent time scale. FIG. 10 shows the contour plots of spatial cross-correlation coefficient of temperature gradient at the position r=0.6. It is confirmed that the burst with long timescale in the case [D] with q0=1.5 has quite large correlation length.

FIG.10. Contour plots of cross-correlation coefficient: $\rho_{x,x=0.6}(\tau) \equiv R_{x,0.6}(\tau)\big/\left(R_{0.6,0.6}(0)R_{xx}(0)\right)^{1/2}$ about L_T^{-1}.

The important things are, this kind of oscillation appears depending on the magnetic shear, and the variation starts from q-minimum region as clearly shown in FIG. 10. The analysis of the triggering mechanism is still in progress. It will be presented in the conference.
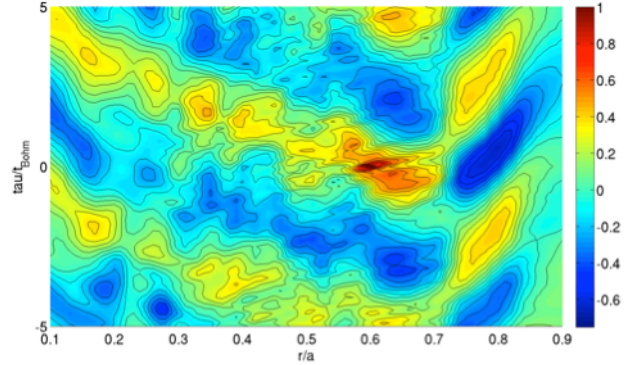
4. Summary

We have investigated magnetic shear effect on ITG turbulence in fully nonlinear regime by the use of global gyro-fluid code. Off-resonant modes around q-minimum region are investigated.

1. It is found that toroidal mode coupling plays a dominant role in the nonlinear regime even around the q-minimum region. Until the nonlinear saturation, the toroidal mode coupling effect on off-resonant modes is relatively weak for the flat shear case. However, it becomes gradually large in the nonlinear saturation phase, and finally the envelope of toroidal ITG mode including off-resonant modes is developed across the q_minimum region.

2. Two different timescale of zonal flow variation is observed. The small avalanche of zonal flow is related to the zonal field propagation across the q-minimum. The large burst is related to the temperature profile relaxation. The burst starts from q-minimum region, and has a long correlation. Quasi-periodic enhancement of mean ExB flow in vicinity of q-minimum followed by the burst is observed.

Acknowledgement

References

[1]   KOIDE, Y., et. al., "Internal transport barrier on q=3 surface and poloidal plasma spin up in JT-60U high βp discharges.", Phys. Rev. Lett. 4 (1978) 3662.

[2]   ITOH, S.-I., ITOH, K., FUKUYAMA, A., "Physics of edge plasmas in enhanced confinement modes.", J. Nucl. Mater. 220-222 (1995) 117-131.

[3]   CONNOR, J. W., et. al., "A review of internal transport barrier physics for steady-state operation of tokamaks", Nucl. Fusion 44 (2004) R1.

[4]   SHIRAI, H., et.al., "Reduced transport and E_r shearing in improved confinement regimes in JT-60U", Nucl. Fusion 39 (1999) 1713.

[5]   FUKUYAMA, A., et. al., "Theory of improved confinement in high-beta p tokamaks", Plasma Phys. Control. Fusion 36 (1994) 1385.

[6]   KIM, J. Y. and WAKATANI, M., "Negative shear effect on toroidal ion temperature gradient mode", Phys. Plasmas 2 (1995) 1012.

[7]   KISHIMOTO,Y.,et.al.,"Toroidal mode structure in weak reversed magnetic shear plasma and its role in the internal transport barrier", Plasma Phys. Control. Fusion 41 (1999) A663.

[8]   DIAMOND, P. H., et. al., "Zonal flows in plasma - A review". Plasma Phys. Control. Fusion 47 (2005) R35.

[9]   YAGI, M., et. al., "Turbulence spreading in reversed shear plasmas", Plasma Phys. Control. Fusion 48 (2006) A409.

[10]   N. Miyato et.al., "Turbulence Suppression in the Neighbourhood of a Minimum-q Surface Due to Zonal Flow Modification in Reversed Shear Tokamaks", Nucl. Fusion 47 (2007) 929.

[11]   CROMBE, K., et. al., "Poloidal Rotation Dynamics, Radial Electric Field, and Neoclassical Theory in the Jet Internal-Transport-Barrier Region", Phys. Rev. Lett. 95 (2005) 155003.

[12]   DE VRIES, P. C., et. al., "Internal transport barrier dynamics with plasma rotation in JET", Nucl. Fusion 49 (2009) 075007.

[13]   IDOMURA, Y., et. al., "Slablike ion temperature gradient driven mode in reversed shear tokamaks", New J. Phys. 4 (2002) 101.1

[14]   TOKUNAGA, S., et. al., "Multi-scale transport simulation of toroidal momentum source profile effect on internal transport barrier collapse", Nucl. Fusion 49 (2009) 075023

[15]   BEER, M. A. and HAMMETT, G. W., "Toroidal gyrofluid equations for simulations of tokamak turbulence", Phys. Plasmas 3 (1996) 4046.

[16]   OTTAVIANI, M. and MANFREDI, G., "The gyro-radius scaling of ion thermal transport from global numerical simulations of ion temperature gradient driven turbulence", Phys. Plasmas 6 (1999) 3267.

[17]   CHANG, Z. and CALLEN, J. D., "Unified fluid/kinetic description of plasma microinstabilities. Part I: Basic equations in a sheared slab geometry", Phys. Fluids B 4 (1992) 1167.

[18] CALLEN, J. D. and SHAING, K. C. "A pressure-gradient-driven tokamak "resistive magneto- hydrodynamic" instability in the banana-plateau collisionality regime". Phys. Fluids 28 (1985) 1845.

[19] GARBET, X., et. al., "Global simulations of ion turbulence with magnetic shear reversal", Phys. Plasmas 8 (2001) 2793.